Computers and Concrete, *Vol. 18, No. 4 (2016) 497-511*
DOI: http://dx.doi.org/10.12989/cac.2016.18.4.497

Load and deflection recovery capacities of PSC girder with unbonded PS H-type steel

Jong-Wook Kim[1a], Jang-Ho Jay Kim[*1], Tae-Kyun Kim[2b] and Chi-Won Lee[1c]

[1]School of Civil and Environmental Engineering, Yonsei University, Concrete Structural Engineering Laboratory, Seoul 03722, Republic of Korea
[2]Hong G Inc, Sunae-ro 46 gil, Bundang-gu, Seongnam-si, Gueonggi-do, Republic of Korea

(Received May 30, 2016, Revised July 25, 2016, Accepted August 12, 2016)

Abstract. Generally, a precast prestressed concrete (PSC) beam is used as girders for short-to-medium span (less than 30 m) bridges due to the advantages of simple design and construction, reduction of construction budget, maintenance convenience. Recently, bridge construction industries have strived to develop a most cost-competitive bridge with longer span. To develop a new type of long span bridge, PSC hollow box girder with H-type steel beam placed at the compressive region is proposed to develop a PSC bridge with a span of more than 50 m. The unbonded compressive prestressing in the H-type steel beams in the girder is made to recover plastic deflection of PSC girder since releasing the pre-stressing. A quasi-static 3-point bending test with 4 different loading steps is performed to verify safety and plastic deflection recovery of the girder. The experimental results showed that the maximum applied load exceeded the maximum design load and most of the plastic deflection was recovered when the compressive prestressing of H-type steel beams is released. Also using prestressed H-type steel as compression reinforcements in the upper part of cross section, repair and restoration difficulty and cost of PSC girders should be significantly reduced. The study result and analysis are discussed in detail in the paper.

Keywords: PS H-type top steel; IT girder; long span girder; real size test; PSC girder

1. Introduction

After the Second World War, the construction of precast prestressed concrete (PSC) girder bridge has drastically increased due to rapid growth in prestressed concrete member popularity, construction easiness from standardized design, significant construction cost reduction by precast construction, durability enhancement from better controlled manufacturing process, etc. Especially in Korea, construction for short to medium span bridges (span with less than 35 m [114.83 ft.]) uses precast PSC girder type. Since 1998, the publication (Ministry of Land, Infrastructure and Transportation 2016) indicates that 44% of the total numbers of bridges connecting Korean express highways are constructed using PSC Girder bridges. Presently, most of 25~35 m

[*]Corresponding author, Professor, E-mail: jjhkim@yonsei.ac.kr
[a]Ph.D. Student: jwkim@kaia.re.kr
[b]Chief Executive Official, E-mail: ceo@hgdcs.com
[c]Master Student, E-mail: hyperior@nate.com

http://www.techno-press.org/?journal=cac&subpage=8 ISSN: 1598-8198 (Print), 1598-818X (Online)

[82.02~114.83 ft] span concrete bridge constructions use concrete with 28 day compressive strength exceeding 40 MPa [5.80 ksi] to manufacture PSC girders. Recently, the publications (Precast/Prestressed Concrete Institure 2003, Oh and Chae 2001, Lee *et al.* 2008, Hindi *et al.* 1995) indicate that its standardized span length has increased up to 45 m [147.64 ft] due to improvements in design and construction technologies. Recently, the prominent PSC girder bridge types of IPC (Han, M. Y. et al), SCP, NE Bulb-T girder (Barow *et al*. 1997) etc have been invented to achieve longer span length in PSC girder bridges. However, the major road block in these advanced PSC girder bridges is that the improvements are only slight modifications from their philosophical origin of high strength concrete utilization, step-wise prestressing technique, and I-type cross-sectional shape. Due to the minor modifications made from previously utilized practices, a great advancement in bridge technology has been lacking in PSC girder bridge design. Also, a major structural problem in using I-type cross-section shape for a girder with span length greater than 45 m [147.64 ft] is large deflection and vibration that can occur due to its relatively low cross sectional stiffness, resulting in long term serviceability problem. For this reason, various steel-concrete composite PSC bridges with low girder height-to-depth ratio and span length up to 50 m [164.04 ft] have been developed. A representative type of a steel-concrete composite bridge is pre-flex member, which was developed in late 1980's and became a trend setter in composite bridge industry. However, the major drawback in steel-concrete composite bridge is its high manufacturing cost where the girder mainly uses H-type steel beam cast with concrete as outer cover, which is extremely expensive when steel cost is high as is the case presently [8]. Also, as the emerging markets' and nations' demands for raw steels dramatically increase (i.e., China and India), the supply for steel becomes limited and is difficult to obtain, resulting in increased construction time and cost.

In Korea, the publications (Jeon *et al*. 2009) are considered most of long span bridges (i.e., span length of 45~60 m [147.64~196.85 ft]) are constructed as steel or PSC box girder bridges (Jeon 2009). Since these bridge types have longer single span length, they are advantageous in application to longer bridges, reflected by many past construction projects. However, since box girder bridges have high cross-sectional height-to-width ratio, they are relatively unstable in lateral direction and prone to structure torsion problems. In order to solve these problems, a bridge type with a single span length of 50~60 m [164.04~196.85 ft] and a low cross-sectional height-to-width ratio is receiving great interests from the bridge industry. Therefore, in this study, a PSC girder called "Intelligent Technology (IT) Girder" that can overcome the limitations of mid to long span PSC girders presently used in construction is proposed and evaluated. The construction process of IT Girder is as same as any precast PSC girders except that it contains unbonded prestressed compression steel members placed at top of its cross-section (compressive region). The placement of compression steel members can achieve 2 main objectives. One is greater compressive stresses can be resisted by the steel members, resulting in reduction of overall height of cross-section. The other is a release mechanism of unbonded prestressing of the compressive steel members, allowing recovery of residual plastic strain or deflection of the member after long term usage of the girder which makes the maintenance of the girder much more simple and economical. IT Girder allows construction of 50~70 m [164.04~229.66 ft] single span PSC girder bridge with decreased cross-section height-to-width ratio without requiring any extra cost, time, construction machinery, and procedure. Also, the recovery of plastic deformation or strain allows savings in cost and time after initial cracking or setting problems, making IT Girder attractive. In order to verify the load carrying capacity and detail failure mechanisms of IT Girder, 50 m [164.04 ft] single span specimen was tested. In this paper, the results obtained from the experiment and Finite Element

Analysis (FEA) simulation of the behavior of IT Girder are discussed in detail.

2. Objective

Due to the relatively heavy self-weight of concrete girder bridges, PSC bridge constructions have been limited to short-to-medium span types with span lengths less than 40 m. The recent bridge construction trend toward rapid precast member constructions by maximizing the length of a single span has required PSC bridges to have a span length over 50~60 m. However, when a PSC bridge has a span length greater than 50~60 m, the height and self-weight of the bridge become too large for construction implementation. Therefore, the objective of this study is to minimize the height, self-weight, and construction cost of PSC girders with a span length greater than 50 m. To achieve these goals, unbonded pre-compressed I-type steel members were placed on the top flange section of the PSC box girder to resist compressive stresses and to recover plastic deflection. The performance verification results of the PSC box girder with a span length greater than 50 m and a height of 2.1 m showed that an innovative PSC girder system can achieve the desired span length and recover some of the plastic deflection during its service state.

3. Research significance

The PSC girder bridges with small or medium span length have been recognized as one of the most economical bridge structure due to the limit of span length and bridge height. Thus, the bridges designed with over 50m (164.04') span length have been mainly constructed as either PSC or steel box girder bridges. In this study, the PSC girder bridge is intended to be designed with less girder weight and lower bridge height for the purpose of increasing span length. The results obtained from this study are utilized as database for the effort to increase the span length of bridge design and to reduce repair and maintenance cost.

4. Concept of IT girder

There are numerous publications related to the longer span length implementation in the bridge girder by improving section configuration with respect to structural design. On the basis of this design philosophy, the girders usually used in the short span bridge (35m) are modified to use them in the long span bridge (50m to 60m). The IT girder presented in this paper can reduce its self-weight and cross sectional height by placing H-type steel beam in the flange section of its

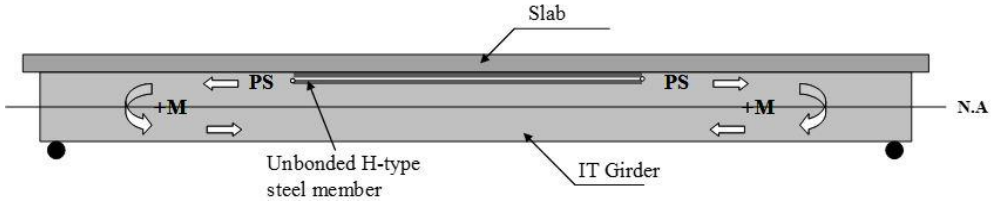

Fig. 1 Applied prestressing and load mechanism

Table 1 Applied prestressing force

Composition	No. of tendon (EA)	Type	Jacking pre-stressing force, kN (kips)	Initial pre-stressing force (kN)
Girder	6 (SWPC 7B-φ15.2-19EA-6EA)	Bonded	3,415.30(767.79) kN/EA	2615.65 (588.02) kN/EA
H-type steel	4×2=8 (SWPC 7B-φ15.2-2EA-8EA)	Unbonded	155.34 (34.92) kN/EA	139.81 (31.43) kN/EA

hollow section configuration. IT girder is expected to have upgraded section stiffness from using unbonded prestressed H-type steel beams. When the compressive prestressing in the H-beams are removed, the plastic deflection can be partially recovered. Fig. 1 shows the technical characteristics of the developed IT girder for a new conceptual design.

5. Experimental method

The load carrying capacity and failure behavior of an actual size IT Girder with 50 m [164.04 ft] single span length are experimentally evaluated in this study. In order to only evaluate the girder capacity, a girder without top slab is tested. The 3-point load test setup is used to induce flexural failure. Initially, a load is applied until tensile cracks are observed in the bottom surface, then the load is removed. Then, the unbonded pre-stressing of H-type steel compression members is released to verify the plastic deflection recovery. Finally, the specimen is reloaded until its maximum capacity is reached or ultimate failure occurs.

5.1 Design of IT girder

The IT girder is designed based on the allowable stress design (ASD) method to satisfy the allowable stress condition. Therefore, concrete stress calculated at both top and bottom concrete slab sections must be less than allowable stress limit. The design live loads were simulated based on the 1st grade DB-24 bridge load requirement. The material parameters (i.e., elastic modulus, creep, and shrinkage) that are usually used to estimate the stress of concrete are used as typical values presented in the design guidelines (Ministry of Construction and Transportation 2010). 6 tendons with 19 steel wires for each tendon are used. Anchorages of the tendons are evenly distributed at two end sections. 8 unboned tendons with 16 steel wires for each tendon are used to apply compressive prestressing force to 2 H-type steel beams placed at the flange section of the IT girder.

D13 and D16 deformed steel rebars are used as shear and flexure reinforcements, respectively, in the IT girder. The reinforcement ratio is 0.0075. Prestressing forces applied to H-beams and tendons are tabulated in Table 1. The cross section, steel reinforcement, tendon details are presented in Fig. 2.

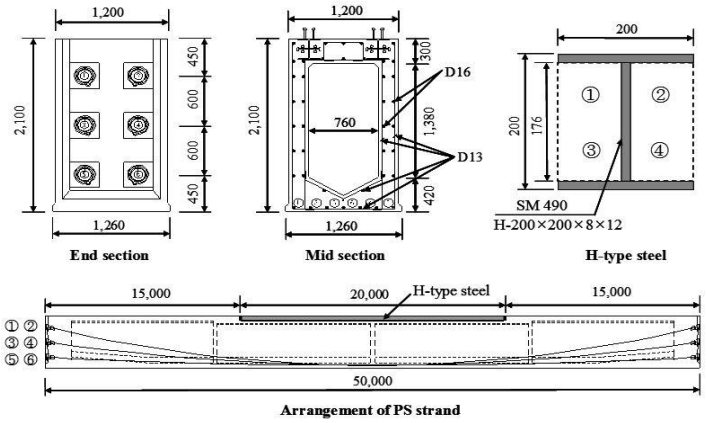

Fig. 2 Sectional dimensions, reinforcing rebar, and PS strand arrangement (unit: mm)

Table 2 Material properties of the test specimen

Material	Young's modulus, GPa (ksi)	Yield stress, MPa (ksi)	Ultimate stress , MPa (ksi)	Compressive strength, MPa (ksi)	Tensile strength, MPa (ksi)	Remark
Concrete	27.2 (3,945.03)	-	-	35 (5.08)	3.8 (0.55)	Design strength
H-type steel	200 (29,007)	320 (46.41)	500 (71.52)	-	-	SM490
PS strands	200 (29,007)	1,600 (232.06)	1,900 (275.57)	-	-	SWPC 7B- φ15.2
Reinforcing bar	200 (29,007)	300 (43.51)	-	-	-	D13, D16

5.2 Specimen characteristics

Initially, IT Girder specimen for the test was designed to have 60 m [196.85 ft] single span. However, due to testing facility constraints in Korea, the span length was reduced to 50 m [164.04 ft]. Since the main objective of the experiment is to verify the load carrying capacity of IT Girder, the specimen is designed based on the requirements of Korean Road and Transportation Design (Ministry of Land, Transport and Maritime Affairs 2010). Also, the construction process of IT Girder exactly followed the procedure used in an actual bridge construction. The test was performed at the laboratory in Korean Institute of Construction Technology in Ilsan, Korea. Since the real size IT Girder was too large to be constructed outside and crane lifted to the load platform, the specimen was constructed on the platform, inside of a laboratory building. Since the center span cross section of the IT Girder specimen is designed to be hollow, the Styrofoam in wedge shape is used to create a hollow center as shown in Fig. 3(b). The wedge shaped Styrofoam is fixed by lever bolts on both sides to prevent it from uplifting during concrete casting as shown in Fig. 3(c). The specimen is constructed indoor using steel assemblage formwork system with concrete design compressive strength of 45 MPa [6.53 ksi]. The specimen as a whole piece is steam cured and the properties of the material used in constructing of the specimen are shown in Table 2. At the time of prestressing, the measured average concrete compressive strength was 35 MPa [5.08 ksi]. The concrete compressive strength was 10 MPa [1.45 ksi] less than the expected strength at the time of prestressing is due to time constraints resulting from constructing the specimen on the indoor loading platform. However, since the lower compressive strength test

(a) Rebar fabrication and sheath tube layout (b) Styrofoam for hollow section (c) Hollow section Styrofoam fixation

(d) H-type steel placement (e) Prestressing of H-type steel (f) Concrete casting

(g) Prestressing of girder (h) Constructed IT girder

Fig. 3 IT Girder construction procedure

result would be more conservative than the actual strength results, the experiment is allowed to continue.

5.3 Load application and data acquisitions

IT Girder was loaded with 3-point loading setup with simple hinge-roller supports. The centre load was applied with H-type steel member, bisecting the member in longitudinal direction. An actuator used for the test was a hydraulic type with 3,000 kN [674.43 kips] maximum capacity. A load was applied as stroke control with 0.02 mm/sec [0.00079 in./sec]. As stated before, the objective of the test is to measure the load carrying capacity and the plastic strain recovery. Therefore, the application of load was divided into 4 loading steps as shown in Table 3. In step 1, the load is applied until the tensile crack is observed at the bottom tensile face of the specimen. In

Table 3 Applied load procedure

Load step	Particular
Step 1	Loading until the initial tensile crack
Step 2	Unloading
Step 3	Remove the compressive pre-stressing of H-type steel
Step 4	Reloading until failure

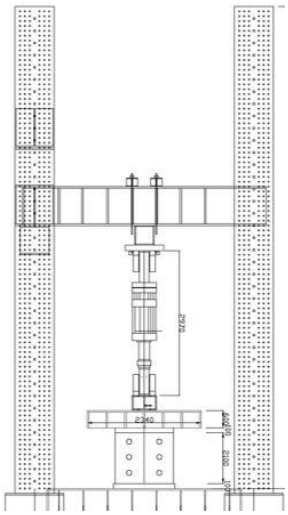

(a) Lateral view

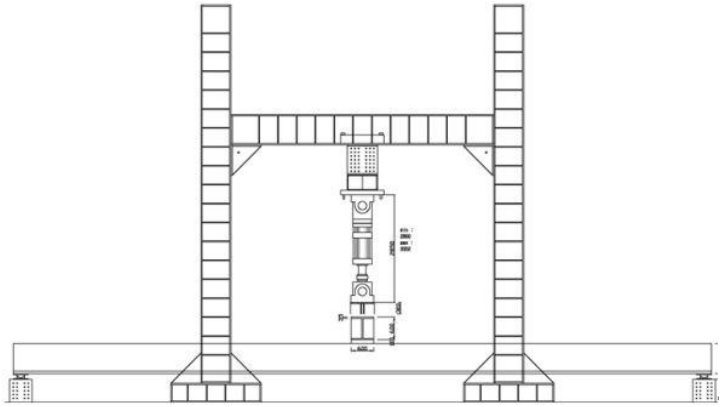

(b) Longitudinal view

Fig. 4 Flexure test setup (unit: mm)

step 2, the load is removed and the specimen is unloaded. In step 3, the unbonded pre-stressing of the H-type steel compressive member is released and plastic strain is allowed to dissipate. Finally, in step 4, the specimen is reloaded until failure. The schematic drawings of the test setup with respect to lateral and longitudinal views are shown in Figs. 4(a) and 4(b), respectively.

In order to acquire strain data of the reinforcements in the specimen during testing, multiple strain gauges are attached to the H-type compressive steel member and the tensile longitudinal

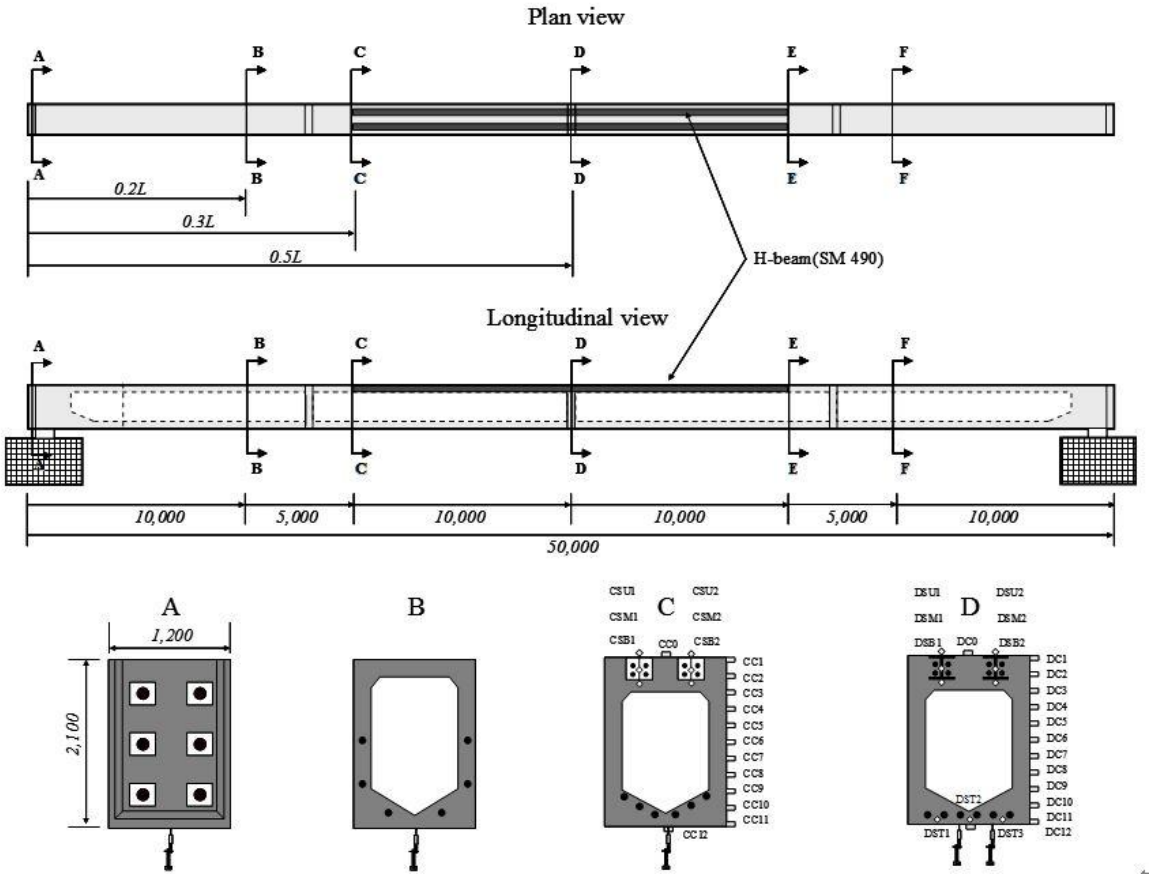

Fig. 5 Test specimen cross-section details and gauge placement locations (unit: mm)

reinforcements before concrete casting. The strain gauges used for the strain data acquisition are made by Japanese company, Tokyo Sokki and Linear Variable Differential Transformers (LVDTs) are used to measure vertical deflections. The LVDTs are placed at 4 locations titled A, B, C, and D as shown in Fig. 5. Also, strain gauge placement locations for the steel reinforcements and the specimen side concrete surface for A, B, C, and D are shown in Fig. 5

6. Experimental results and discussions

6.1 Load-vertical deflection behavior

The measured applied load versus vertical deflection experimental results for the locations of 0.5L(centre), 0.3L, and 0.2L are shown in Figs. 6(a), 6(b), and 6(c), respectively. In the load step 1, with the stroke controlled loading rate of 0.02 mm/sec [0.00079 in./sec], the initial tensile crack occurred at the load of 1,615 kN [363.07 kips] with the centre deflection of 187 mm [7.4 in.]. When the load is removed to let the specimen unload in the load step 2, the residual centre

Table 4 Applied load versus vertical deflection results at various locations

Load step	Applied load , kN (kips)	Deflection, mm (in.)		
		0.5L (center)	0.3L	0.2L
Step 1	1,615 (363.07)	187.0 (7.4)	148.7 (5.85)	106.2 (4.18)
Step 2	0 (0)	18.7 (0.74)	15.5 (0.61)	11.04 (0.43)
Step 3	0 (0)	7.7 (0.3)	7.0 (0.28)	5.2 (0.2)
Step 4	2,000 (449.62)	246.8 (9.72)	195.2 (7.69)	139.5 (5.49)

Table 5 Design and experimental value comparison

Load step	Load, kN (kips)		Deflection, mm(in.)
	Design	Experiment	
Service load	980 (220.32)	-	-
Cracking load	1,260 (283.26)	1,615 (363.07)	187.0 (7.4)
Ultimate load	3,000 (674.43)	2,000 (449.62)	246.8 (9.72)

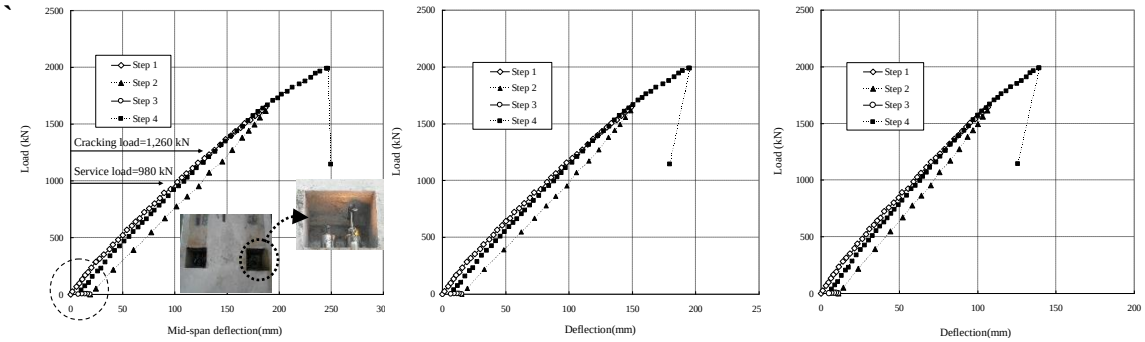

(a) D section (Mid-Span, 0.5L) (b) C section (0.3L) (c) B section (0.2L)

Fig.6 Load-deflection curve for the load steps

deflection was 18.7 mm [0.74 in.]. In the load step 3, when the compressive pre-stressing of the unbonded H-type steel compressive member is released by cutting the bolt fixture using a torch fire, 11 mm [0.43 in.] of the residual deflection is recovered as shown in Fig. 6(a). Therefore, after the load step 3, the total residual deflection at the centre of specimen was 7.7 mm [0.3 in.]. This recovery indicates that the recovery mechanism using unbonded pre-stressing of the compression members is working. In the load step 4, the specimen is reloaded using a stroke controlled loading rate of 0.02 mm/sec [0.00079 in./sec] until failure. At the load of 1,400 kN [314.73 kips] in reloading stage, the load-deflection curve crosses the original loading curve, indicating recovery of original stiffness from crack closing. As the reloading continued and reached 2,000 kN [449.62 kips], the top H-type steel compressive member abruptly debonded, causing catastrophic failure of the specimen. The abrupt debonding failure can be originated from the less than expected concrete compressive strength, causing reduction of concrete bond strength (e.g., design concrete

compressive strength of 45 MPa [6.53 ksi] was actually 35 MPa [5.08 ksi] at testing due to an insufficient curing time) and a lack of confinement effect due to the absence of top slab.

The vertical deflections at LVDT locations of 0.3L and 0.2L at the crack initiation load of 1,615 kN [363.07 kips] were 148.7 mm [5.85 in.] and 106.2 mm [4.18 in.], respectively. After the unbonded pre-stressing of H-type steel compression member was released, the residual deflections at 0.3L and 0.2L were 7.0 mm [0.28 in.] and 5.2 mm [0.2 in.], respectively, with the associated deflection recoveries of 8.5 mm [0.33 in.] and 5.84 mm [0.23 in.], respectively. As shown from the vertical and residual deflection results, the deflection recoveries decrease as data acquisition location moves away from the centre of the specimen. Table 4 shows the summary of the load-deflection results for all of the load steps. The experimental results are summarized in Table 5, as compared with the design results concerning service loads, crack loads, ultimate loads, and defections. For crack loads, the design result is 1260kN, and more conservative than the experimental result having 1615kN. As shown in Fig. 6 (a), the experimental specimen has 980kN for the service load, and thus there is no problem for serviceability. The crack load obtained from the experimental test is 1.7 time larger than 980kN design load including the impact factor, meaning that the experimental specimen do not generate any crack even under the service load. Furthermore, the experimental specimen just arrives at 35MPa less than 45MPa design strength for the ultimate state, and thus has additional resistance strength to accommodate more external forces. Therefore, if the experimental specimen is constructed with high strength concrete, structural safety will ameliorate, and this will be adequately applied to the long span bridge with 50-60m span length.

6.2 Load-strain and concrete strain results

Figs. 7(a), 7 (b), and 7 (c) show top and bottom surfaces' load-strain results for the locations D (centre, 0.5L), C (0.3L), and E (0.7L), respectively. These data are obtained from top and bottom surface attached strained gauges for each load increment. As shown in Fig. 7(a), the maximum allowable concrete compressive strain of 0.003 did not occur when the ultimate failure load was reached. The maximum load and compressive strain at failure were 2,000 kN [449.62 kips] and 0.0011, respectively. The specimen showed no sign of concrete compressive failure. As stated before and shown in Fig. 7(a), the initial hairline tensile crack appeared at the load of approximately 1,615 kN [363.07 kips]. This load exceeded the cracking design load of 1,300 kN

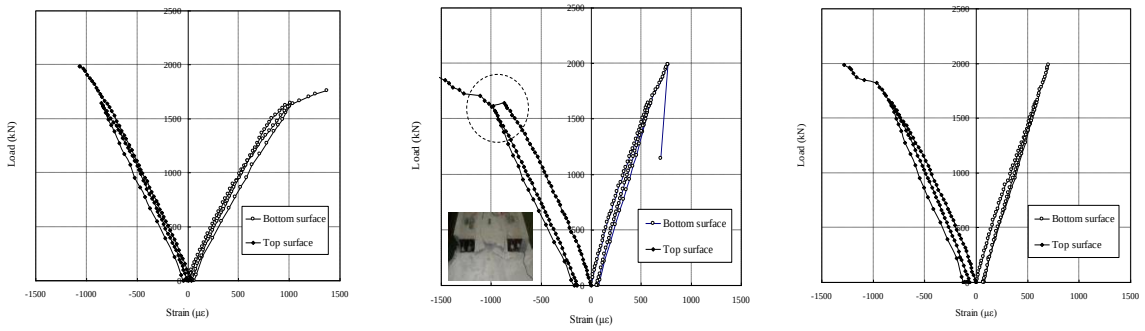

(a) D section (Mid-Span, 0.5L) (b) C section (0.3L) (c) E section (0.7L)

Fig. 7 Load-strain results at top and bottom surface

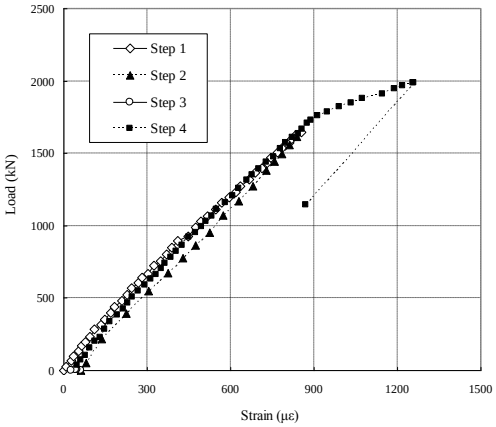

Fig. 8–Load-strain relationship of tensile reinforcement at the center span
(Note: 1 kN = 0.2248 kips; 1 mm = 0.0394 in.)

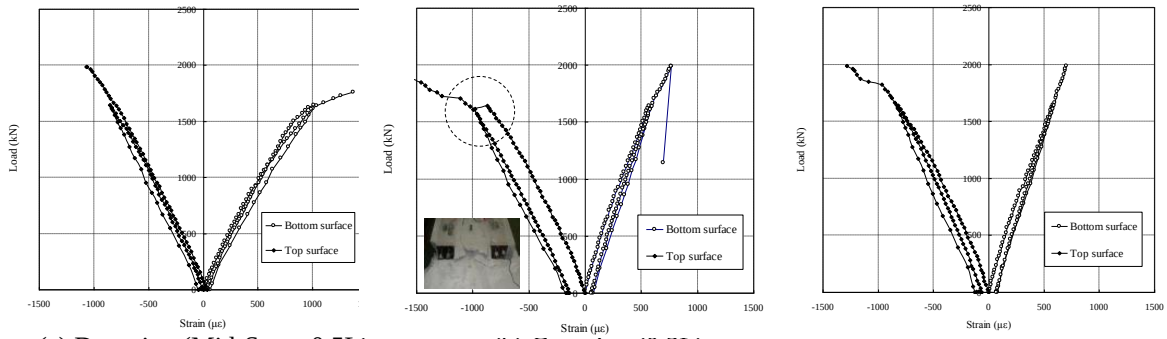

(a) D section (Mid-Span, 0.5L) (b) C section (0.3L) (c) E section (0.7L)

Fig. 9 Load-strain relationship at the H-type compressive steel member

[292.25 kips], showing an ample crack resistance capacity of IT Girder. However, at location C, the concrete compressive failure has occurred at the top compressive region of the specimen as shown in Fig. 7(b). The dotted circle in Fig. 7(b) indicates the time when the interface failure between concrete and H-type steel member in the top section occurred. The abrupt change in load-strain behavior is indicating the interface failure. However, due to the interface failure, plastic deflection was not recovered at the locations C and E when the unbonded pre-stressing is released, unlike the recovery of the center location D.

6.3 Tensile longitudinal reinforcement strain results

The load-strain relationship results obtained from the tensile longitudinal reinforcements at the centre of the specimen is shown in Fig. 8. As the results indicate, the initial crack formation time is more precisely reflected in this data than the strain data obtained from concrete surface. When the initial cracks formed at the load of 1,615 kN [363.07 kips], the sudden increase in strain incremental values occurs for load increments. However, the load carrying capability is still intact even though the stiffness of specimen is noticeably degraded. Therefore, as the results indicate, the

safety of IT Girder exceeds the design requirements and ductile failure behaviour is insured. The experimental results verify that IT Girder's concept of reducing section height by implementing compressive steel member is working, thereby increasing constructability and cost efficiency.

6.4 H-type compressive steel member strain results

Figs. 9(a), 9(b), and 9(c) show load strain relationship results obtained from strain gauges attached at top, middle, and bottom of cross section at the locations of D (centre, 0.5L), C (0.3L), and E(0.7L), respectively. In Fig. 9(a), the H type compressive steel member is in compression throughout the loading step 1.

Even when the load is removed and the specimen is unloaded in the loading step 2, the residual deflection is not significant. When the unbonded prestressing is released in the loading step 3, the member goes into tension with largest and smallest tensile stresses at top and bottom surfaces, respectively. However, the deflection recovery is not significant. At C and E locations, the H type compressive steel member is in compression during initial loading then gradually transforms into tension during the loading step 1. After the load is removed and the specimen is unloaded in the loading step 2, significant residual deflections existed at C and E locations, unlike location D. Also, when unbonded prestressing is released in the loading step 3, the deflection recovery is significant at C and E locations, unlike location D. The results indicate that the effect of the prestressing release is more significant further away from the centre and more near H steel member concrete interface.

7. Verification of experimental results

7.1 FE modeling characteristics

Analytical simulation of IT Girder flexure test was undertaken for two specific reasons. One is to nearly understand the idealistic failure behaviour of the test since the specimen prematurely

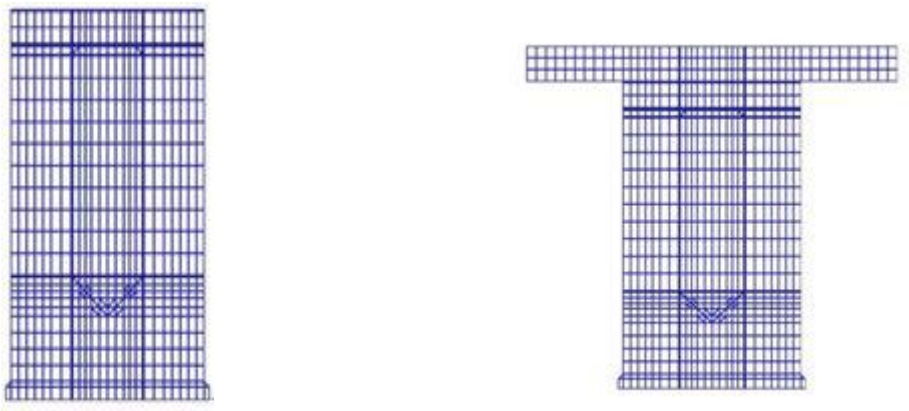

(a) IT girder without slab (b) IT girder with slab

Fig. 10 FE modeling

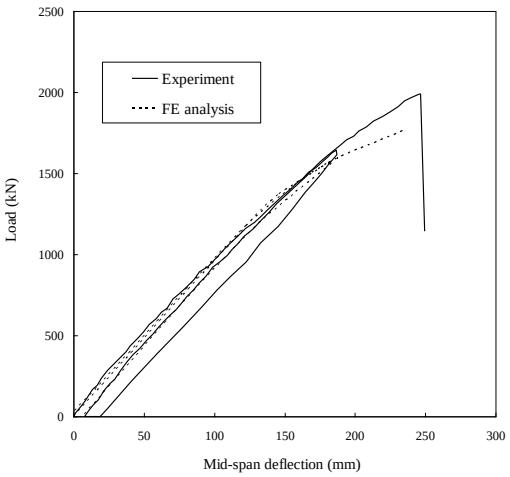

Fig. 11 Simulation and experimental result comparison

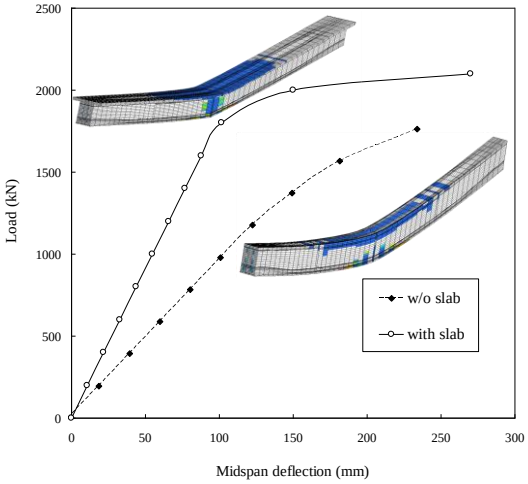

Fig. 12 FE simulation results

failed due to debonding failure of the H type compressive steel member. Second is to prepare a tool for future design of IT Girders when dimensions and materials need to be varied. Third, the confined effect of the IT girder, which is generated by installing the upper slab, is intended to be investigated. It is not considered during the experimental test. Since the scope of the analytical simulation is not developing analysis method or tool for IT Girder, a commercial FEM code of DIANA was used to perform nonlinear simulation of IT Girder flexure test. The FEM model consisted of solid concrete X section, hollow concrete X section, H type compressive steel member, pre stressing tendon, and reinforcing bar. The concrete section and H type steel member were modeled using 8 node rectangular and 6 node triangular solid elements. The prestressing tendon and reinforcing bar were modeled using embedded elements. The material models used for concrete and steel were Drucker Prager and von Mises failure criteria, respectively. Fig. 10 shows the mesh of IT Girder analytical model. The load steps used in the analysis were exactly same as the experiment.

7.2 Comparison of analysis and experimental results

Fig. 11 shows the force and deflection curve measured at the centre of the girder in the comparison of analysis result and experimental result. After observing analysis results, the bottom of the IT girder is subjected to compression force immediately after applying pre-stressing, while the top of the IT girder is under tension force. The maximum camber of 111mm takes place in the middle point. The initial crack takes place under 1200kN loading along the contact line between steel and concrete, and the tension crack is also observed at this loading stage. The bearing failure caused by pre-stressing is also observed at both end support because the IT girder is constructed with 35MPa concrete strength less than 45MPa design strength. On the other hand, as shown in Fig. 10, the analysis result shows a good agreement with the experimental result until 1600kN.

After removing the load, the residual deformation obtained from the analysis result is smaller than that from the experimental result. This trend of the analysis result is due to the condition that

contact surfaces between steel and concrete are assumed to be fully adhesion. The recovery capacity for the performance of the IT girder can be affirmed by removing the pre-stressing of the upper steel member in that recoverable displacement is 76mm, which exist due to the removal of upper compression pre-stress. The IT girder fails by 1800kN underestimated by 2000kN from the experimental test result. However, the analysis result that takes structural safety into consideration show a similar agreement with the experimental result in term of entire response. Fig. 12 shows analytical comparisons between IT girders according to the existence of the upper slab. The IT girder with the upper slab has 2100kN ultimate strength while that without the upper girder has 1800kN ultimate strength. The IT girder with the upper slab showed 20mm larger displacement in the middle point than that without the upper slab. The upper slab provides upgraded stiffness capability to the IT girder due to the expansion of the girder section. It is finally concluded based on the analysis result that the IT girder with the upper slab show better performance than that without the upper slab

8. Conclusions

To evaluate the practical applicability of the IT girder developed for long span PSC girders, a static performance evaluation test was carried out on an actual girder of 50m single span length, and the following conclusions are derived.

IT Girder showed a very stable linear behaviour in service load conditions. Although concrete with strength that was much lower than design strength of 45 MPa [6.53 ksi] was used due to insufficient curing time, it nevertheless showed a high load carrying capacity of approximately 2,000 kN [449.62 kips]. If concrete with design strength of 45 MPa [6.53 ksi] is used and the H type compression steel member is confined by the presence of upper slab, the capacity will improve additionally.

The introduction of the additional compressive stress in the lower part of the girder from the removal of unbonded pre-stressing of the H-type compression steel members showed a capacity improvement of approximately 60% (7.7 mm [0.3 in.]) recovery of the residual plastic deflection (18.7 mm [0.74 in.]), showing that the plastic deflection recovery using unbonded pre-stressing works. By using this recovery system, repair and rehabilitation of PSC girder should be easier and less costly.

The developed IT Girder is expected to have a very low girder height (2.1 m [6.89 ft]) for the span length (50~60 m [164.04~196.85 ft]). With addition of weight reduction using a hollow cross section, the girder can be extended even up to 70~80 m [229.66~262.47 ft] span length with proper adjustments.

The developed IT Girder can be safely applied to the existing PSC girder bridges with maximum span of 35~60 m [114.83~196.85 ft], replacing existing steel girder bridges and PSC box girder bridges. Also, it is expected to be widely utilized in the future as a next generation's mid to long span girder bridges that can reduce construction cost and time.

The FE analysis result showed 1800kN ultimate strength, which is 90% level of the experimental result (i.e., 2000kN ultimate strength). If the upper slab is installed at the IT girder, ultimate strength will increase to 2100kN due to an additional stiffness, upgrading the performance of the IT girder.

Acknowledgements

This work was supported by the Nuclear Safety Research Program through the Korea Foundation of Nuclear Safety (KOFONS), granted financial resource from the Nuclear Safety and Security Commission (NSSC) of the Republic of Korea (No. 1403010). Also, this work was partially supported by the Yonsei University Future-Leading Research Initiative of 2015 (2015-22-0122).

References

Bardow, A.K., Seraderian, R.L. and Culmo, M.P. (1997), "Design, fabrication and construction of the New England Bulb-Tee girder", *PCI J.*, **42**(6), 30-40.

Han, M.Y., Hwang, E.S. and Lee, C. (2003), "Prestressed concrete girder with multistage prestressing concept", *Struct. J.*, **100**(6), 723-731.

Hindi, A., MacGregor, R., Kreger, M.E. and Breen, J.E. (1995), "Enhancing strength and ductility of post-tensioned segmental box girder bridges", *ACI Struct. J.*, **92**(1), 33-44.

Jeon, S.J. (2009), "Assessment for extending span ranges of PSC girder bridges: II. Application to a sample bridge", *J. Korean Soc. Civil Eng.*, **29**(3A), 243-250.

Jeon, S.J., Choi, M.S. and Kim, Y.J. (2009), "Assessment for extending span ranges of PSC girder bridges: I. Proposed strategy to estimate the spans", *J. Korean Soc. Civil Eng.*, **29**(3A), 235-241.

Lee, S.C., Feng, M.Q., Hong, S.H. and Chung, Y.S. (2008), "Long-term monitoring and analysis of a curved concrete box-girder bridge", *Int. J. Concrete Struct. Mater.*, **2**(2), 97-98.

Ministry of Land, Infrastructure and Transportation (2016), *Yearbook of Bridge Statistics*. Ministry of Land, Infrastructure and Transportation, Sejong, South Korea.

Ministry of Land, Transport and Maritime Affairs (2010), *Korean Road and Transportation Design*. Korea Road and Transportation Association, Seoul, South Korea.

Oh, B.H. and Chae, S.T. (2001), "Structural behavior of tendon coupling joints in prestressed concrete bridge girders", *Struct. J.*, **98**(1), 87-95.

Precast/Pre-stressed Concrete Institure (2003), "Precast Pre-stressed Concrete Bridge Design Manual." 2nd Edition, PCI, Chicago, 2003.